Biochemistry

 Volume 39, Number 31 August 8, 2000

Articles

Kinetic Scheme for Intermolecular RNA Cleavage by a Ribozyme Derived from Hepatitis Delta Virus RNA†

I-hung Shih and Michael D. Been*

Department of Biochemistry, Duke University Medical Center, Durham, North Carolina 27705

Received March 3, 2000; Revised Manuscript Received May 31, 2000

ABSTRACT: A minimal kinetic mechanism for a *trans*-acting ribozyme derived from the HDV antigenomic RNA self-cleaving element was established from steady-state, pre-steady-state, single-turnover, and binding kinetics. Rate constants for individual steps, including substrate binding and dissociation, cleavage, and product release and binding, were measured at 37 °C at pH 8.0 in 10 mM Mg^{2+} using oligonucleotides as either substrates, noncleavable analogues or 3′ product mimics. A substrate containing a normal 3′,5′-linkage was cleaved with a first-order rate constant (k_2) of 0.91 min^{-1}. The association rate constant for the substrate to the ribozyme (2.1×10^7 M^{-1} min^{-1}) was at the lower range of the expected value for RNA duplex formation, and the substrate dissociated with a rate constant (1.4 min^{-1}) slightly faster than that for cleavage. Thus the binary complex was not at equilibrium with free enzyme and substrate prior to the cleavage step. Following cleavage, product release was kinetically ordered in that the 5′ product was released rapidly (>12 min^{-1}) relative to the 3′ product (6.0×10^{-3} min^{-1}). Rapid 5′ product release and lack of a demonstrable binding site for the 5′ product could contribute to the difficulty in establishing the ribozyme-catalyzed reverse reaction (ligation). Slow release of the 3′ product was consistent with the extremely low turnover under steady-state conditions as 3′ product dissociation was rate-limiting. The equilibrium dissociation constant for the substrate was 24-fold higher than that of the 3′ cleavage product. A substrate with a 2′,5′-linkage at the cleavage site was cleaved with a rate constant (k_2) of 1.1×10^{-2} min^{-1}. Thus, whereas cleavage of a 3′,5′-linkage followed a Briggs-Haldane mechanism, 2′,5′ cleavage followed a Michaelis−Menten mechanism.

Self-cleaving sequences found in hepatitis delta virus (HDV)[1] liberate single copies of linear RNAs from replication intermediates in both the genomic and antigenomic strands (*4*−*6*). The minimal wild-type sequence for robust autocatalytic activity is 84 nt 3′ and one nt 5′ to the cleavage site in both ribozymes (*7*, *8*). The two ribozymes share ∼75% sequence identity and assume a similar secondary structure consisting of a nested double-pseudoknot fold (*9*, *10*).

The HDV ribozymes catalyze cleavage of a 3′,5′-phosphodiester bond via nucleophilic attack of the adjacent 2′-hydroxyl group on the scissile phosphorus, generating a 2′,3′-cyclic phosphate and a 5′-hydroxyl terminus (*5*, *6*). Details of the chemical mechanism remain to be established, but recent evidence suggests that proton-transfer involving C76 of the antigenomic ribozyme (C75 in the genomic) is important for cleavage activity (*9*, *11*, *12*). Divalent metal ions are also required for efficient activity (*5*−*7*, *13*, *14*) and are likely involved in cleavage chemistry. The HDV ribozyme can also cleave a 2′,5′-linked phosphodiester bond

† This work was supported by NIH Grant GM47233.

* To whom correspondence should be addressed. Phone: (919) 684-2858. E-mail: been@biochem.duke.edu.

[1] Abbreviation: HDV, Hepatitis delta virus; Tris, tris(hydroxymethyl)-aminomethane; EDTA, (ethylenedinitrilo)tetraacetic acid; bp, base-pair; nt, nucleotide or nucleotides; PEI, poly(ethyleneimine); TLC, thin-layer chromatography.

10.1021/bi000499+ CCC: $19.00
Published on Web 07/08/2000

by an analogous mechanism in that a cyclic phosphate is generated (*15*). However, 2′,5′ cleavage has an altered divalent metal ion preference, providing further evidence for an essential role of metal ions in HDV cleavage.

Even though the in vivo cleavage activity of naturally occurring HDV ribozymes is encoded in a single RNA molecule, intermolecular cleavage can be achieved by dividing the autocatalytic sequence into two parts, a *trans*-acting ribozyme and a substrate. These two sequences associate through base-pairing to reconstitute catalytic activity (*16*−*20*). Conversion to intermolecular cleavage reactions has facilitated the mechanistic and structural studies of other ribozymes (see refs *21*−*23* for reviews). For the HDV ribozymes, the cleavage rate constant for single-turnover has been reported and partial kinetic schemes have been proposed (*16*, *24*−*26*). However, rate constants for individual steps in a complete minimal kinetic scheme have not yet been determined for intermolecular cleavage. A detailed kinetic scheme would provide a foundation for further mechanistic understanding of HDV ribozyme catalysis. We have elucidated a complete cleavage kinetic scheme for a HDV *trans*-acting antigenomic ribozyme ADC1 (*19*) using a combination of pre-steady-state and steady-state kinetic and equilibrium binding assays. We find that the kinetic mechanism depends on the phosphodiester linkage at the cleavage site. With a 3′,5′-linked substrate, the reaction kinetics follows a Briggs-Haldane mechanism because the dissociation rate constant for the substrate is comparable to that of the chemistry step. However, with a 2′,5′-linked substrate, the chemistry step is extremely slow; therefore, substrate binding is at rapid equilibrium before proceeding to cleavage (a Michaelis−Menten mechanism). Nevertheless, the rate-limiting step for turnover with this ribozyme is release of the 3′ cleavage product for both 3′,5′- and 2′,5′-linked substrates as proposed previously (*15*). These results provide insights into the mechanistic and biological function of the HDV ribozymes and establish a basis for further studies on their mechanism and applications.

MATERIALS AND METHODS

Enzymes, Chemicals, Oligonucleotides, and Plasmids. T7 RNA polymerase (provided by M. Puttaraju) was purified from an overexpressing clone provided by W. Studier (*27*). Restriction endonucleases, nucleotides, ^{32}P-labeled nucleotides, chemicals, reagents, and other enzymes were purchased from commercial suppliers. HDV ribozymes were transcribed from pADC1 (*19*). Plasmid DNA was purified by CsCl/ethidium bromide equilibrium centrifugation.

Oligonucleotide Substrates. The RNA substrates DS3 [5′UUC(3′,5′)GGGUCGG3′], DS2 [5′UUC(2′,5′)GGGUCGG3′], and 3′ cleavage product DP3 (5′GGGUCGG3′) were gifts from Ribozyme Pharmaceuticals, Inc. (Boulder, CO). The noncleavable substrate analogue DSA10 [5′UUdC(3′,5′)GGGUCGG3′], which contains one deoxynucleotide 5′ to the cleavage site, was purchased from Dharmacon Research, Inc. (Boulder, CO).

5′-End labeled substrate RNA was prepared using polynucleotide kinase and [γ-^{32}P]ATP (*19*). 3′-End labeled substrate RNA was prepared using T4 RNA ligase and [5′-^{32}P]pCp (*7*). Labeled oligonucleotides were purified on 20% polyacrylamide gels.

Preparation of RNAs. The HDV ribozyme ADC1 was prepared from plasmid DNA linearized with *Hin*dIII by in vitro transcription with T7 RNA polymerase (*19*). Following transcription, RNA was purified by electrophoresis on a 6% polyacrylamide gel under denaturing conditions. RNA was eluted from gel slices and passed through gel-filtration columns (Sephadex G-10 for oligonucleotides and G-25 for ribozyme ADC1; Pharmacia), ethanol precipitated, and resuspended in dH_2O. Concentrations of RNA were estimated from the base composition and extinction coefficients at 260 nm. RNA was stored at −20 °C, and aliquots were heated to 95 °C for 1 min immediately before use.

Pre-Steady-State and Single-Turnover Experiments. For cleavage reactions, the ribozyme and substrate were preincubated in buffer 1, containing 40 mM Tris-HCl (pH 8.0) and 1 mM EDTA, at 37 °C for 10 min, and the reaction was started by addition of $MgCl_2$ to yield "standard conditions" [40 mM Tris-HCl (pH 8.0), 1 mM EDTA, and 11 mM $MgCl_2$ at 37 °C; buffer 2]. Aliquots were taken at various time points, quenched with an equal volume of 0.1 M EDTA, and fractionated on PEI plates in 1 M LiCl (*15*). The fraction cleaved was visualized and quantified using a PhosphoImager (Molecular Dynamics). First-order rate constants (k_{obs}) were obtained from data fit to a single-exponential equation (eq 1) using the KaleidaGraph data analysis/graphics application (Synergy Software):

$$[P]_t = [P]_\infty(1 - e^{-k_{obs}t}) \quad (1)$$

where k_{obs} is the first-order rate constant; $[P]_t$, and $[P]_\infty$ are the fraction cleaved at time t and the end point, respectively. At least three independent data sets were collected, and variation was 20% or less. The reported errors in the text are asymptotic standard errors obtained from curve-fitting.

Pulse-Chase Experiments To Determine Dissociation and Association Rate Constants of the Substrate, k_{-1} and k_1. For determining k_{-1}, excess ribozyme and a trace amount of labeled substrate (<1 nM) were preincubated in buffer 1 at 37 °C, and the reactions were started by addition of $MgCl_2$ to yield standard conditions. At time t_1, unlabeled substrate or product oligonucleotide in buffer 2 was added to the reactions. At time t_2, the reactions were terminated with an equal volume of 0.1 M EDTA. For k_1, the conditions were similar except the ribozyme and substrate were preincubated separately in buffer 2 at 37 °C, and the reactions were initiated upon mixing. Fractionation and quantification were performed as described above. Time t_1 and t_2 varied among chase experiments and are specified in individual sections of the Results.

Steady-State Experiments. Steady-state experiments were carried out in multiple-turnover reactions with excess substrate to ribozyme ([S]/[E] ≥ 5) under standard conditions. Reactions were initiated, terminated, and quantified as described for the single-turnover experiments.

Gel-Shift Assay. Gel-shift assays were used for measuring the dissociation rate constants and equilibrium dissociation constants of substrate and product oligonucleotides. Nondenaturing gels contained 10% acrylamide (acrylamide-to-bisacrylamide ratio of 29:1, w/w), 50 mM Tris-acetate (pH 7.5), and 10 mM magnesium acetate. The running buffer contained 50 mM Tris-acetate (pH 7.5) and 10 mM magnesium acetate. Aliquots were loaded directly to the gels at each time point while the electric field was applied. Elec-

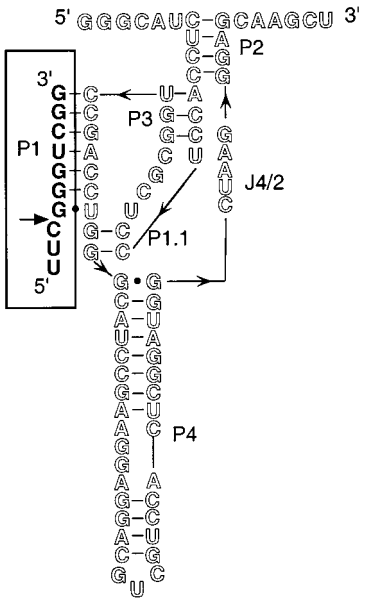

FIGURE 1: Sequence and secondary structure of the ADC1 ribozyme and its substrate. The sequence of the *trans*-acting ribozyme is shown in outlined letters. The substrate is boxed and shown in solid letters, with the cleavage site, between the third (C) and fourth (G) nucleotides, indicated by an arrow.

trophoresis was carried out at low current (20 mA) to prevent disruption of the complex as a result of warming of the gel.

Gel Filtration Columns. A centrifuge column packed with Sephadex G-10 was used to measure the dissociation of the 5′ cleavage product from the ribozyme. This procedure was performed as described (*3*).

RESULTS

The *trans*-acting HDV ribozyme, ADC1, used in this study (Figure 1) was derived from the antigenomic sequence (*19*). A minimal kinetic mechanism for the intermolecular cleavage reaction of the HDV ribozyme under "standard conditions" [40 mM Tris-HCl (pH 8.0), 1 mM EDTA, and 11 mM $MgCl_2$, at 37 °C] is summarized in Figure 2. The mechanism includes substrate association (k_1) and dissociation (k_{-1}), cleavage (k_2), and product release (k_3 and k_4) and binding (k_{-4}). The approaches used in this kinetic characterization of the HDV ribozyme were adapted from those used in previous studies of catalytic RNAs (*3*, *28*−*30*).

Pre-Steady-State Cleavage. The pre-steady-state parameters were first determined under single-turnover conditions in the presence of excess ribozyme ([E]/[S] ≥ 5). The ribozyme and substrate were preincubated in buffer 1 at 37 °C for 15 min, and the cleavage reactions were started by addition of $MgCl_2$. Aliquots were quenched with an equal volume of 0.1 M EDTA at various time points and separated by thin-layer chromatography (TLC). Under these conditions, the cleavage reaction can be described by Scheme 1 (*3*), in

Scheme 1

$$E + S \underset{k_{-1}}{\overset{k_1}{\rightleftharpoons}} E{\bullet}S \xrightarrow{k_2} E + P_{3'} + P_{5'}$$

which the ribozyme/product ternary complex ($E{\bullet}P_{5'}{\bullet}P_{3'}$) is disrupted by addition of EDTA and the separation process. Therefore, product release is not observable. Time courses were fit to a single first-order exponential (eq 1). The observed rate constants (k_{obs}) were measured in reactions containing various concentrations of ribozyme (4−1000 nM) and a trace amount of 5′-end labeled oligonucleotide substrate DS3 (<1 nM) (Figure 3A). The observed pseudo-first-order rate constants (k_{obs}) were plotted as a function of ribozyme concentration (Figure 3B) and fit to eq 2:

$$k_{obs} = \frac{k_2[E]_{tot}}{K_M' + [E]_{tot}} \quad (2)$$

The maximum first-order rate constant at the saturating ribozyme concentration, k_2, is 0.91 ± 0.02 min^{-1}, and the concentration of ribozyme at which the reaction rate is half-maximal, K_M', is 110 ± 10 nM. These two parameters give a second-order rate constant, k_2/K_M', of (8.3 ± 0.2) × 10^6 M^{-1} min^{-1}. At low concentrations of ADC1 ribozyme (4−32 nM), the observed rate constants increased linearly with the ribozyme concentration (Figure 3B, inset). This linear dependence gave a slope of (7.5 ± 0.5) × 10^6 M^{-1} min^{-1}. The values of k_2/K_M' calculated by these two methods were in good agreement.

The pre-steady-state parameters were also determined under substrate excess conditions. The observed cleavage rate constants for the first-turnover (the burst rate for the first molar equivalent of product to enzyme, *P*/*E*) were measured as described above (data not shown). Under these conditions, k_2 and K_M' were (0.93 ± 0.11) min^{-1} and (138 ± 15) nM, respectively, which were very close to the values obtained in the single-turnover reactions.

Partition of E·S between Dissociation and Cleavage. To examine the partition of the E·S complex between substrate dissociation and the chemistry step, pulse-chase experiments were carried out under single-turnover conditions (*31*). As outlined in Scheme 2, excess ribozyme (E, 500 nM) and a trace amount of 5′-^{32}P-labeled substrate (S*) were used in the partition reaction so that a maximal amount of S* was bound to the ribozyme rapidly. At various times t_1, the E·S* complex was then challenged by addition of excess unlabeled product oligonucleotide DP3 ([P]/[E]$_{tot}$ ≥ 10), which binds to free ribozyme rapidly and inhibits further association of the labeled substrate to the ribozyme. The

Scheme 2

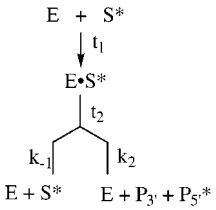

chase reactions were then quenched with EDTA after chase period t_2 (30 min), allowing the bound substrate to react to completion. Control reactions were quenched with EDTA directly at time t_1. The fraction cleaved was plotted against t_1 and fit to a single exponential (Figure 4). For each t_1, the extent of cleavage in the chase reaction was higher than that of the control reaction, but lower than the end point of the control reaction, indicating that a portion of the bound substrate did not go on to cleave but instead dissociated from the binary complex. Raising the concentration of ribozyme

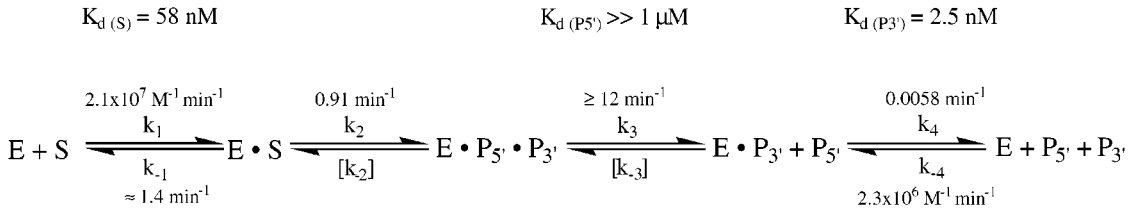

FIGURE 2: The minimal kinetic scheme for cleavage by ADC1 at 37 °C in 11 mM $MgCl_2$, 40 mM Tris-HCl (pH 8), and 1 mM EDTA (standard conditions). E, ADC1 ribozyme; S, substrate oligonucleotide DS3; $P_{5'}$, 5′ cleavage product; $P_{3'}$, 3′ cleavage product. The equilibrium and rate constants determined are indicated next to individual steps. Constants in brackets were not determined in this study.

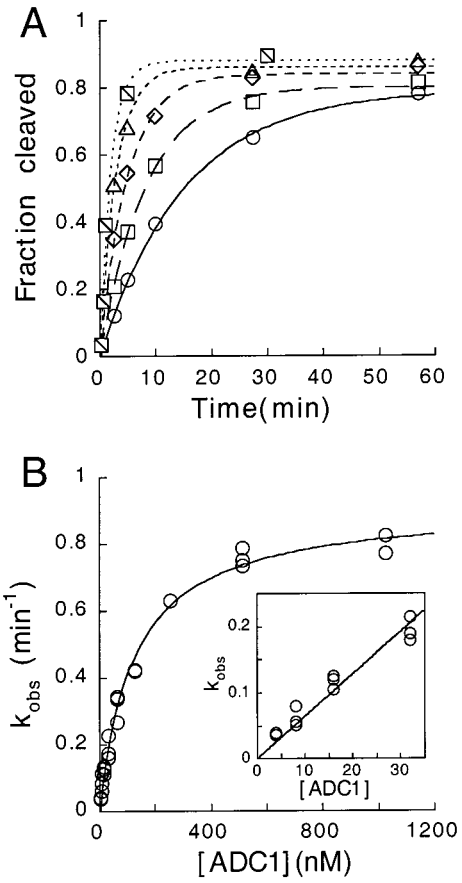

FIGURE 3: Single-turnover cleavage reactions with trace amounts of substrate and varying concentrations of excess ribozyme under standard conditions. (A) Cleavage time courses at 8 (○), 16 (□), 32 (◇), 64 (△), and 256 (open box with slash) nM ADC1 ribozyme were fit to a single-exponential. (B) Observed pseudo-first-order rate constants are plotted against ribozyme concentration. The first-order rate constant for the chemistry step (k_2) is 0.91 ± 0.02 min^{-1}, and the concentration at half-maximum rate (K_M') is 110 ± 10 nM. The inset shows the linear dependence of the rate constants on lower concentrations of ribozyme with a slope of (7.5 ± 0.5) × 10^6 M^{-1} min^{-1}.

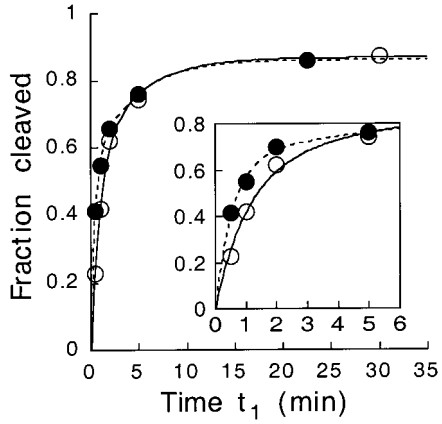

FIGURE 4: Partitioning of the E•S complex assayed by pulse-chase experiments. Single-turnover ADC1 cleavage reactions contained a trace amount of substrate (<1 nM) and ribozyme at saturating concentration (500 nM). The control reaction (○) was quenched with an equal volume of 0.1 M EDTA at the indicated times (t_1). The product trap reaction (●) was first quenched with an equal volume of excess product oligonucleotide DP3 at 36 μM at the indicated times (t_1), followed by addition of an equal volume of 0.1 M EDTA after 30 min. Both sets of data were plotted against time t_1 and fit to a single-exponential. The inset shows early time points. The minimal dissociation rate constant of the substrate was estimated from the first time point (30 s) to be 1.1 min^{-1}.

to 1 μM or the chase period (t_2) to 60 min in the pulse-chase experiments gave essentially the same results (data not shown), confirming that the maximal E•S* complex was formed before the chase and that the chase reaction reached completion under these conditions. The dissociation rate constant of the substrate (k_{-1}) was estimated to be ≥1.1 min^{-1} from the first time point (30 s) using eq 3:

$$[P]_{30s,chase}/[P]_{\infty,control} = k_2/(k_2 + k_{-1}) \qquad (3)$$

where $[P]_{30s,chase}$ is the fraction of S* cleaved in the chase reaction after t_2 (t_1 = 30 s) and $[P]_{\infty,control}$ is the end point of the control reaction. This value sets the lower limit for k_{-1} because the E•S* complex might reach the maximal amount before the first time point (30 s). However, these data indicated that pre-steady-state cleavage did not follow a Michaelis−Menten kinetic mechanism because the rate constant for substrate dissociation (k_{-1}) is comparable to the cleavage rate constant (k_2). Thus, the E•S complex did not reach equilibrium before proceeding to the chemistry step. In addition, the rate-limiting step under substrate subsaturating conditions (k_2/K_M') is not simply substrate association (k_1) but a combination of k_1, k_{-1}, and k_2, because k_2 is only slightly slower than k_{-1}.

Dissociation Rate Constant of the Substrate. To measure the dissociation rate constant of the substrate, the partitioning experiments were modified slightly. Excess ribozyme and a trace amount of labeled substrate were used in the cleavage reaction. Cleavage proceeded for time t_1 (30 s), at which excess unlabeled product was added to the reaction. Following the chase period t_2 (15 s to 10 min), aliquots of the reaction were quenched with EDTA. The control cleavage reaction was carried out under the same conditions but without the chase. The fraction cleaved was plotted against (t_1 + t_2) for both the control and chase reactions (Figure 5A). The dissociation rate constant (k_{-1}) was determined in the following two ways.

First, k_{-1} was calculated using the end point ($[P]_\infty$) of the control and chase reactions. The extent of cleavage of the

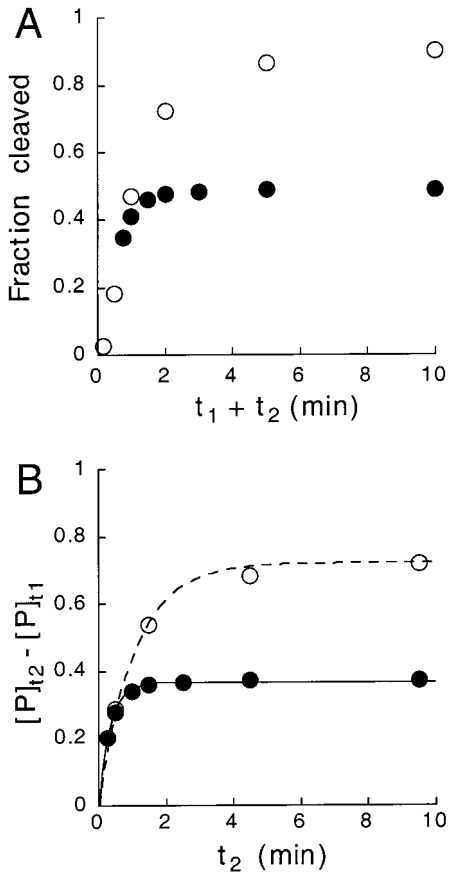

FIGURE 5: Determination of the substrate dissociation rate constant from pulse-chase experiments. The experiments were carried out as outlined in Scheme 2. (A) ADC1 (0.5 μM) and a trace amount of substrate were allowed to react for 30 s (t_1), followed by either the addition of unlabeled DP3 [chase (●)], or allowed to continue without chase [control (○)]. Reactions were quenched with an equal volume of 0.1 M EDTA at t_2. The fraction cleaved was plotted against ($t_1 + t_2$). The end points for the chase and control reactions were 49 and 92%, respectively. (B) The fraction cleaved after t_1 ($[P]_{t_2} - [P]_{t_1}$) was plotted against time t_2. The pseudo first-order rate constants obtained from the chase and control reactions were 2.1 and 0.87 min^{-1}, respectively. The substrate dissociation rate constant calculated from panels A and B gave a value of 1.3 and 1.2 min^{-1}, respectively (see text).

chase reaction after initial substrate binding time t_1 is proportional to the partitioning between k_2 and k_{-1} according to eq 4:

$$([P]_{\infty,\text{chase}} - [P]_{t_1,\text{control}})/[E\cdot S]_{t_1} = ([P]_{\infty,\text{chase}} - [P]_{t_1,\text{control}})/([S]_{\text{tot}} - [P]_{t_1,\text{control}}) = k_2/(k_{-1} + k_2) \quad (4A)$$

This relation is based on the assumption that all of the substrate is bound to the ribozyme at the initial time t_1. However, for the ADC1 ribozyme, 5−15% of the substrate was not cleaved in the single-turnover reactions. Therefore, eq 4A was modified as follows:

$$([P]_{\infty,\text{chase}} - [P]_{t_1,\text{control}})/([P]_{\infty,\text{control}} - [P]_{t_1,\text{control}}) = k_2/(k_{-1} + k_2) \quad (4B)$$

in which $[P]_{\infty,\text{control}}$ is the end point of the control reaction. The dissociation rate constant of the substrate calculated from this equation was 1.1−1.6 min^{-1}.

The second method of calculation makes use of observed rate constants (k_{obs}). The pseudo-first-order rate constants of the chase ($k_{\text{obs,chase}}$) and control ($k_{\text{obs,control}}$) reactions after t_1 were obtained from single-exponential fit to the plot of ($[P]_{t_2} - [P]_{t_1}$) against t_2 (Figure 5B). The cleavage rate of the chase reaction is faster than that of the control reaction because E·S decays via parallel pathways of substrate dissociation

Scheme 3

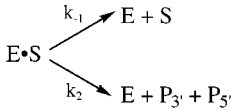

and the chemistry step (Scheme 3). The dissociation rate constant was calculated using eq 5:

$$k_{\text{obs,chase}} = k_2 + k_{-1} \quad (5)$$

in which k_2 is the rate constant of the control reaction ($k_{\text{obs,control}}$) under ribozyme saturating conditions. The value of k_{-1} calculated by this method was 1.1−1.4 min^{-1}.

k_{-1} was also determined by following dissociation of the E·S complex directly with a gel-shift assay using a noncleavable substrate analogue, DSA10, containing a 2′-deoxynucleotide at the cleavage site. The maximal amount (>80%) of binary complex $E\cdot S_{\text{analogue}}$ was preformed under standard conditions for 30 min and excess product oligonucleotide DP3 was added to block further association of DSA10 to the ribozyme. Decay of the $E\cdot S_{\text{analogue}}$ complex was followed on a nondenaturing gel. By this method, a lower limit for the dissociation rate constant was estimated to be 1 min^{-1} (data not shown).

There are two possible artifacts from pulse-chase experiments which could cause overestimation on the dissociation rate constants. One is due to incomplete binding before addition of cold product oligonucleotide DP3 at time t_1. Varying the time t_1 (15−45 s) and ribozyme concentration (500−2000 nM) rendered essentially the same value of k_{-1}. Therefore E·S complex formation already reached maximum before the chase. Another potential artifact arises from the assumption of a one-step binding mechanism. A more complicated binding mechanism involved in basepair formation of the substrate and enzyme in P1 followed by a conformational change (e.g., helix docking), as seen with L-21 ScaI ribozyme derived from the *Tetrahymena* group I intron (*32*), could result in overestimation of the overall dissociation rate constant of the substrate (Scheme 4).

Scheme 4

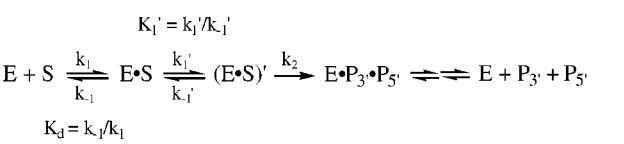

However, the overestimation would only occur if the k_1' is much slower than k_{-1}, which is unlikely the case for the ADC1 ribozymes (see Discussion). In addition, the dissociation rate constant obtained from the pulse-chase experiments was consistent with the number determined independently using gel-shift assay with a 2′-deoxy substrate analogue,

suggesting the number determined based on a simple one-step binding kinetics was reasonable.[2]

Association Rate Constant of the Substrate. The second-order rate constant k_2/K_M' (8.2×10^6 M^{-1} min^{-1}) was a combination of substrate association, dissociation and cleavage [$k_2/K_M' = k_1k_2/(k_{-1} + k_2)$], thus, the rate constant of substrate binding, k_1, was calculated to be 2.1×10^7 M^{-1} min^{-1}. This value was confirmed by pulse-chase experiments. To follow accumulation of the E·S complex, relatively low concentrations of ribozyme (but still in excess of substrate, [E]/[S] $\geq$ 5) were used. The amount of total E·S complex that has formed over the interval t_0 to t_1 ($[E\cdot S]_{t_0-t_1}$) is equal to the amount of cleavage product plus the amount of E·S complex present at t_1 (Figure 6A and eq 6A):

$$[E\cdot S]_{t_0-t_1} = [P]_{t_1} + [E\cdot S]_{t_1} \quad (6A)$$

Since the amount of E·S complex was difficult to follow directly by gel-shift assays, the amount of product formed ($[P]_\infty$) at the end of the chase period (t_2) was converted to the amount of E·S complex that remained uncleaved at time t_1 ($[E\cdot S]_{t_1}$) by multiplying by a factor of $(k_{-1} + k_2)/k_2$ using the relation in eq 4A (eq 6B):

$$[E\cdot S]_{t_0-t_1} = [P]_{t_1} + ([P]_{\infty,\text{chase}} - [P]_{t_1,\text{control}})(k_{-1} + k_2)/k_2 \quad (6B)$$

Time dependence of the $[E\cdot S]_{t_0-t_1}$ for the two-step reaction, as described by Scheme 1, followed a double-exponential with two observed rate constants (*33*):

$$k_{obs1} \approx k_1[E] + k_{-1} + k_2$$

$$k_{obs2} \approx k_1k_2[E]/(k_1[E] + k_{-1} + k_2) \quad (7)$$

The data for $[E\cdot S]_{t_0-t_1}$ formation were first fit to a double exponential equation $[[E\cdot S]_{t_0-t_1} = a_1 \exp(-k_{obs1}t) + a_2 \exp(-k_{obs2}t)]$, but this failed to render reasonable results due to uncertainty of the amplitude (a_1 and a_2). However, under the reaction conditions used, these two rate constants were well separated (k_{obs2} was at least 10-fold slower than k_{obs1}), and at the early time points the rate constants governing the rise of $[E\cdot S]_{t_1}$ and lag phase of $[P]_{t_1}$ were both k_{obs1}. Therefore the rate constants were determined by fitting the plot of $[E\cdot S]_{t_0-t_1}$ vs time t_1 to a single exponential (Figure 6, panels A and B), which was a close estimate for k_{obs1}. The second-order rate constant, k_1, of $(2.0 \pm 0.1) \times 10^7$ M^{-1} min^{-1} was subsequently obtained from the slope of the plot of k_{obs} against [E] (Figure 6C), which was consistent with the value obtained from k_2/K_M'. The intercept of 0.73 ± 0.09 did not correspond to $k_{-1} + k_2 \approx 2.2$. The discrepancy for the *y*-intercept might result from the assumption of a single- rather than double-exponential fit for k_{obs1} of the E·S complex. This discrepancy was also seen when we compared a single- and a double-exponential fit to a data set generated by KINSIM simulation (*34*). The dissociation and association rate constants determined by pulse-chase experiments gave an equilibrium dissociation constant 55∼70 nM [$K_{d(S)} = k_{-1}/k_1$] for the substrate DS3.

[2] This interpretation is based on the assumption that the 2′-hydroxyl group at the cleavage site is not required for promoting the tertiary docking.

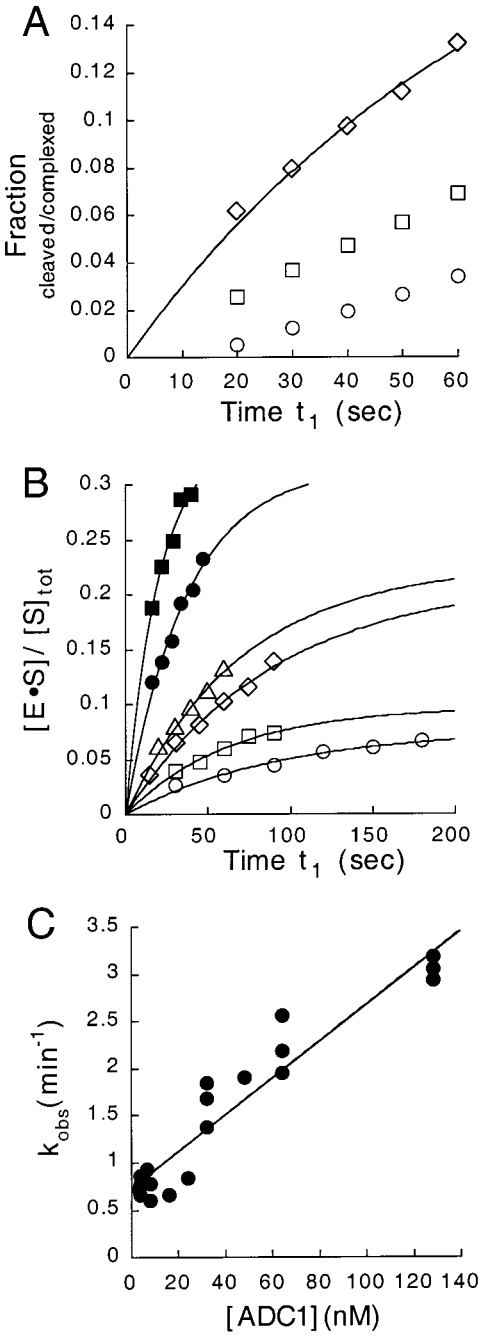

FIGURE 6: Determination of the rate constants for substrate binding. The experiments are outlined in Scheme 2. (A) Pulse-chase experiments with ADC1 ribozyme at 24 nM. The fraction cleaved during t_1 (○), during chase period t_2 (□), and fraction that formed the E·S complex during t_1 (◇), calculated as described in the text, were plotted as a function of time t_1. The observed rate constant (k_{obs}) for accumulation of the E·S complex was obtained by fitting the data to a single exponential. (B) Pulse-chase experiments with ADC1 at low concentrations: 4 (○), 8 (□), 16 (◇), 24 (△), 64 (●), and 128 (■) nM. The amount of E·S complex accumulated was plotted as a function of t_1 and fit to a single exponential. (C) The first-order rate constants obtained from panel B are linearly dependent on ADC1 ribozyme concentration. The slope of $(2.0 \pm 0.1) \times 10^7$ M^{-1} min^{-1} is the rate constant for substrate binding.

Equilibrium Dissociation Constant of the Substrate. The equilibrium dissociation constant of a noncleavable substrate analogue, DSA10, was also measured directly by gel-shift assays. A trace amount of 5′-end labeled DSA10 was preincubated with excess ribozyme at different concentrations under standard conditions for 30 min, and the E·S* complex

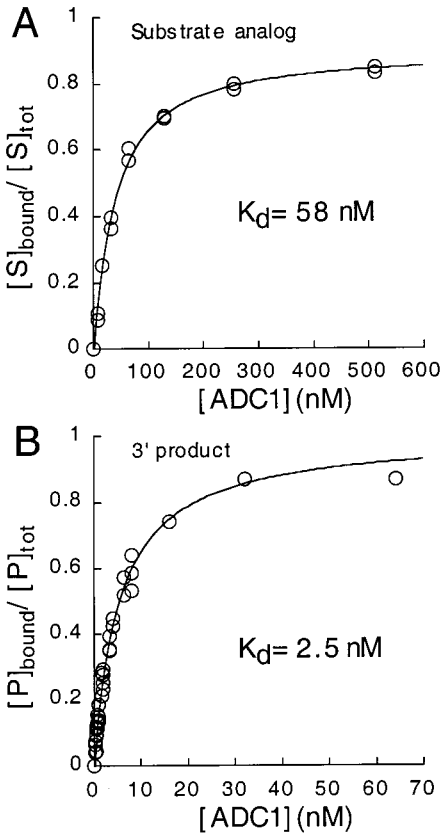

FIGURE 7: Determination of the equilibrium dissociation constants of the substrate analogue DSA10 and the 3′ product DP3. ADC1, at varying concentrations, was mixed with a trace amount of 5′-end-labeled DSA10 (A) or 3′-end-labeled DP3 (B) under standard conditions for 30 min to reach equilibrium. The binary complex was separated from the free oligonucleotide by nondenaturing gel electrophoresis. The fraction bound was plotted against ribozyme concentration and the data were fit to eq 8, giving a K_d of 58 ± 3 and 2.5 ± 0.2 nM for the substrate analogue and 3′ product, respectively.

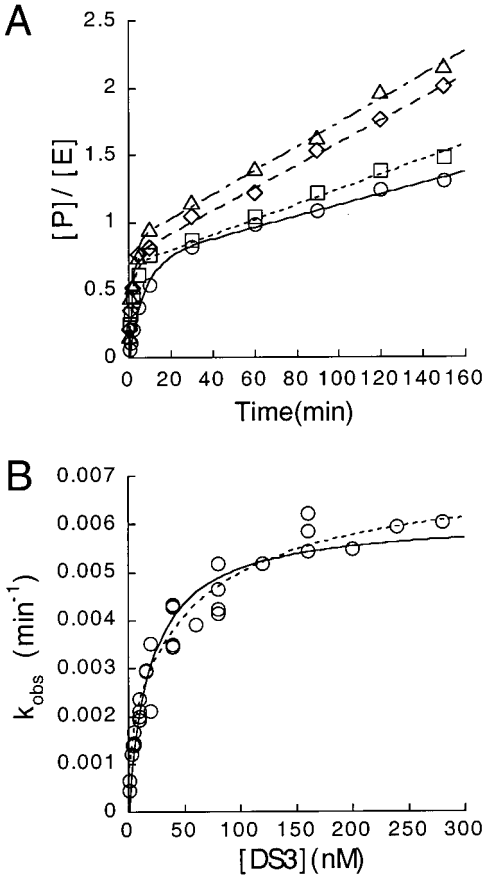

FIGURE 8: Multiple-turnover of ADC1 and the substrate DS3. (A) Time courses of the cleavage reactions done under standard conditions with 4 nM ADC1 ribozyme and excess DS3 at 20 (○), 40 (□), 80 (◇), and 160 (△) nM. Molar ratio of product over ribozyme (P/E) was plotted as a function of time and fit to eq 9, giving a linear phase with a slope ranging from 0.0025 to 0.0053 min^{-1}. The burst amplitude ranged from 75 to 95%. (B) Multiple-turnover parameters of ADC1 cleavage. Cleavage reactions were carried out with excess substrate ([S]/[E] ≥ 5) under standard conditions. The slope of the linear phase following the burst (k_{obs}) was plotted against substrate concentration and data were fit to eq 10 (solid line), giving a maximal rate constant $k_{cat} = (6.1 \pm 0.2) \times 10^{-3}$ min^{-1}, and a Michaelis constant $K_M = 8 \pm 1$ nM. The dotted line represents the fit to $v = (A[S] + B[S]^2)/(C + D[S] + [S]^2)$ (see footnote 5).

and unbound substrate were separated by nondenaturing gel electrophoresis. The equilibrium dissociation constant, K_d, of the substrate analogue of (58 ± 3) nM was determined from the plot of the fraction of bound substrate vs ribozyme concentration (Figure 7A) using eq 8:

$$[S]_{bound}/[S]_{tot} = 1/(1 + K_d/[E]_{tot}) \quad (8)$$

This value obtained from gel-shift assays was in good agreement with that from a competitive inhibition assay under subsaturating conditions ($K_i = 60 \pm 4$ nM) (*15*).

Pre-Steady-State Burst. Biphasic kinetics has been observed for the HDV ribozymes under substrate excess conditions (*16*, *35*). These cleavage reactions showed an initial burst followed by a linear increase of product formation. Multiple-turnover reactions with DS3 were carried out at various concentrations of the substrate in excess to ribozyme ([S]/[E] ≥ 5) and fit to eq 9:

$$\frac{[P]_t}{[E]_{tot}} = k_{obs}t + A(1 - e^{-k_{burst}t}) \quad (9)$$

in which k_{obs}, k_{burst}, and A represent the turnover rate constant, burst rate constant, and burst amplitude, respectively. The data were consistent with a two-step mechanism which indicated a fast chemical conversion followed by a slow step of regeneration of active ribozyme (Figure 8A). The burst amplitude (A) ranged from 75 to 95%, suggesting that a fairly high fraction of the ribozyme population was catalytically active.

The steady-state parameters were determined from a plot of the turnover rate constants as a function of substrate concentration using eq 10 (Figure 8B, solid line):

$$k_{obs} = \frac{k_{cat}[S]_{tot}}{K_M + [S]_{tot}} \quad (10)$$

The turnover number, k_{cat}, and Michaelis constant, K_M, were $(6.1 \pm 0.2) \times 10^{-3}$ min^{-1} and (8 ± 1) nM, respectively ($k_{cat}/K_M = 7.6 \times 10^5$ M^{-1} min^{-1}).

Rate-Limiting Step for Steady-State Kinetics. To determine if product release is the rate-limiting step under substrate saturating conditions, the dissociation rate constants of the products were measured. Cleavage of the substrate DS3

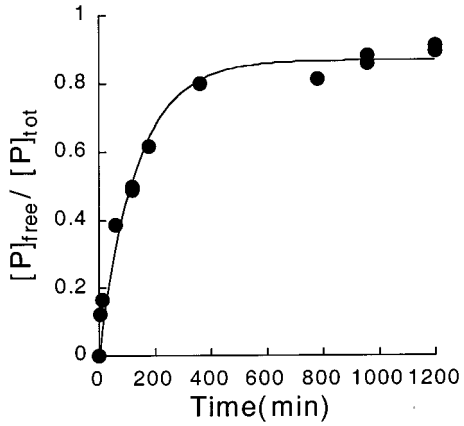

FIGURE 9: The dissociation rate constant of the 3′ cleavage product. The binary complex of ribozyme and labeled 3′ product (E·P*) was allowed to form in buffer 2 at 37 °C for 30 in and then challenged with excess unlabeled product oligonucleotide (chase). The labeled 3′ cleavage product (P*) released from E·P* was followed by native-gel electrophoresis. The fraction of unbound product ($[P]_{unbound}/[P]_{tot}$) was plotted against time after chase and fit to a single exponential, giving a first-order rate constant of $(5.8 \pm 0.5) \times 10^{-3}$ min^{-1}.

generates the 5′ product 5′UUC>P (>P, a 2′,3′-cyclic phosphate), and the 3′ product HO-GGGUCGG3′ (HO-, a 5′-hydroxyl group). Previous studies argued against the possibility that the sequence 5′ to the cleavage site contributed to substrate binding (*19*). In addition, cleavage activity of ADC1 was not inhibited by the presence of the 5′ product (10 nM to 10 μM) at both subsaturating and saturating ribozyme concentrations (A. T. Perrotta and M.D.B., unpublished data). Consistent with these data, we found that 5′ product release was too fast to be measured with either gel-shift assays or centrifuge columns (*3*). The rate constant of 5′ product dissociation was estimated to be ≥ 0.2 s^{-1} from the time for the sample to pass through (transient time) the centrifuge column (10 s) (data not shown).

The dissociation rate constant of the 3′ product (k_4) was determined using gel-shift assays. Excess ribozyme (1 μM) and a trace amount of 3′-end labeled product oligonucleotide[3] DP3 were incubated under standard conditions for 30 min to allow binding to reach equilibrium. Over 85% of the product oligonucleotide was bound to the ribozyme under these conditions. An equal volume of unlabeled DP3 (at 80 μM) were then added and aliquots were removed at various time points and loaded directly onto nondenaturing gels. The fraction of the product dissociated after the chase was corrected for the unbound fraction at time t_0 and plotted against time (Figure 9). The rate constant obtained from a fit to a first-order exponential was $(5.8 \pm 0.5) \times 10^{-3}$ min^{-1}. This number was the same, within error, as the turnover number [$k_{cat} = (6.1 \pm 0.2) \times 10^{-3}$ min^{-1}], demonstrating that the rate-limiting step for turnover is dissociation of the 3′ cleavage product. Dissociation of the 5′ product is much faster than that of the 3′ product, and therefore the kinetically preferred order for product release from the $E{\cdot}P_{3'}{\cdot}P_{5'}$ ternary complex is the 5′ product before the 3′ product (Figure 2).

The equilibrium dissociation constant of the 3′ cleavage product was also determined by gel-shift assays. The conditions were the same as those used for measuring the K_d of the substrate analogue, except that the oligonucleotide DP3 was labeled at the 3′-end (HO-GGGUCGG*pC-p) instead of the 5′-end.[3] The equilibrium dissociation constant determined by this method ($K_d = 2.5 \pm 0.2$ nM; Figure 7B) was in good agreement with the dissociation constant obtained using a competitive inhibition assay (DP3, HO-GGUCGG-OH, $K_i = 2.2 \pm 0.3$ nM; data not shown).[4] The association rate constant (k_{-4}) of the 3′ product obtained from the K_d and k_4 ($k_{-4} = K_d/k_4$) was 2.3×10^6 M^{-1} min^{-1}.

Table 1: Kinetic Parameters of the Substrates DS3 and DS2

	k_2 (min^{-1})	K_M' (nM)	k_2/K_M' (M^{-1} min^{-1})	k_{cat} (min^{-1})	K_M (nM)	k_{cat}/K_M (M^{-1} min^{-1})
DS3	0.91	110	8.3×10^6	0.0061	8	7.6×10^5
DS2	0.011	16	6.6×10^5	0.0028		

Kinetic Mechanism for Cleavage of a 2′,5′-Linked Substrate. Cleavage of a 2′,5′-linkage at the cleavage site has been previously demonstrated with ADC1 (*15*). The similarity in pH profiles between 2′,5′ and 3′,5′ cleavage reactions suggested that the chemistry step is rate-limiting in both cases. To further characterize the cleavage reaction with a 2′,5′-linkage, kinetic parameters of ADC1 cleavage of the 2′,5′-linked substrate, DS2, were determined (Table 1). DS2 shares the same sequence as DS3 but contains a 2′,5′-phosphodiester linkage at the cleavage site. For single-turnover reactions, the first-order rate constant with saturating ribozyme (k_2) was determined to be $(1.06 \pm 0.02) \times 10^{-2}$ min^{-1} (Figure 10A), which was 2 orders of magnitude slower than that of the normal substrate DS3 (Table 1). Pulse-chase experiments were carried out to examine the partitioning of the E·S complex (data not shown). The data suggested that the dissociation of DS2 was much faster than the chemistry step, and, therefore, binding of the substrate is at rapid equilibrium (data not shown). The second-order rate constant (k_2/K_M') obtained from the fit of the plot of k_{obs} vs ribozyme concentration was $(6.62 \pm 0.07) \times 10^5$ M^{-1} min^{-1} (Figure 10A; inset).

Multiple-turnover with DS2 at saturating concentrations also showed burst-kinetics but with a slope for steady-state of $(2.8 \pm 0.3) \times 10^{-3}$ min^{-1} (Figure 10B). The rate of 3′ product dissociation would be expected to be the same (5.8×10^{-3} min^{-1}) because the cleavage reaction of the 2′,5′-linked substrate generates the same 3′ cleavage product as that for the normal substrate (*15*). This value is comparable to the rate constant of chemical conversion; therefore, the overall turnover rate is determined by a combination of two steps as $k_2k_3/(k_2 + k_3) = 3.4 \times 10^{-3}$ min^{-1} (*36*), which is consistent with the measured one. The burst amplitude of the multiple-turnover for DS2 does not simply represent

[3] The 3′ product generated from ADC1 ribozyme cleavage bears a 5′-OH group. Phosphorylation of the 5′-OH resulted in destabilization of the $E{\cdot}P_{3'}$ complex (I.-h.S., and M.D.B., unpublished data). Therefore the oligonucleotide DP3 were 3′-end *pCp labeled instead of 5′-end.

[4] On the basis of free-energy parameters from a nearest-neighbor model (*1*, *2*), the 3′ dangling nucleotide in the RNA duplex could contribute to the stability of 0.4 kcal/mol (equivalent to 2-fold increase in binding affinity). However, the binding constant K_d determined for DP3 (competitive inhibition assay) and the 3′-*pCp-end labeled DP3 (gel-shift assay) were the same within error. Using only gel-shift assay, the contribution of the 3′ dangling cytosine to stability of the binary complex E·S was determined by comparing the dissociation equilibrium constants between the 5′-end and 3′-*pCp-end labeled substrate analogue DSA10. Less than 50% tighter binding was seen with the 3′-*pCp-end labeled DSA10. Therefore, the higher limit for K_d of DP3 was 3.7 nM.

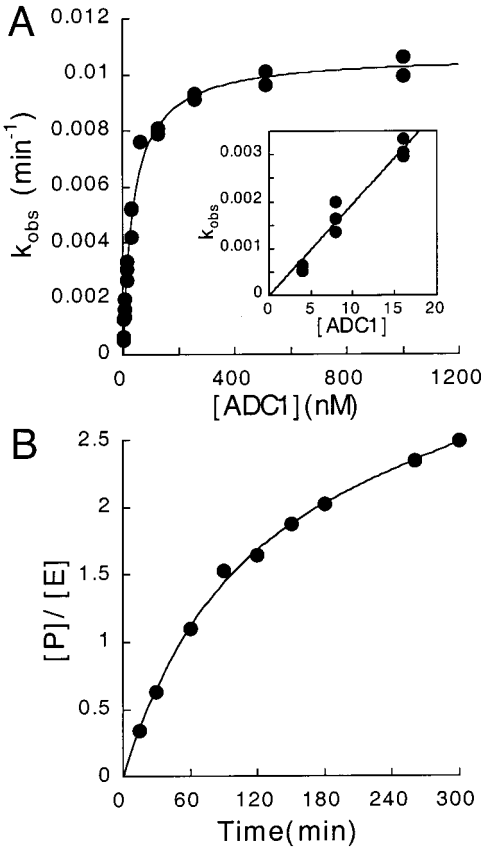

FIGURE 10: Single-turnover and multiple-turnover cleavage of the 2′,5′-linked substrate DS2. (A) Reaction rate constant (k_{obs}) for the 2′,5′-linked substrate DS2 plotted against ribozyme concentration under pre-steady-state conditions. The k_2 and K_M' obtained from the fit of the plot are $(1.06 \pm 0.02) \times 10^3$ min^{-1} and 16 ± 2 nM, respectively. (B) Time course of DS2 cleavage under substrate saturating conditions of 1 μM ([ADC1] = 0.1 μM). The data were fit to eq 9, giving an initial burst amplitude of 51% followed by a linear phase with a slope = $(2.8 \pm 0.3) \times 10^{-3}$ min^{-1}.

stoichiometry of the enzyme concentration, but, instead, is dependent on the ratio of $[k_2/(k_2 + k_3)]^2$ (*36*). The measured burst amplitude of 51% is close to the expected value of 42%.

DISCUSSION

Summary of the Kinetic Mechanism. A kinetic scheme for cleavage reactions catalyzed by a *trans*-acting HDV ribozyme was established by measuring individual elemental rate constants, including cleavage of the phosphodiester bond and association and dissociation of the substrate and product (Figure 2). In multiple-turnover reactions, the substrate binds to the ribozyme to form the E·S complex, which partitions between the chemistry step and substrate dissociation with a relative ratio of 1:1.6 (k_2: k_{-1}). The portion that goes on to the chemistry step generates two cleavage products (5′ and 3′ products). These two products dissociate from the ribozyme in a kinetically ordered pathway because the dissociation rate constant of the 5′ product is at least 2×10^3 fold faster than that of the 3′ product. Dissociation of the 3′ product, which is 140-fold slower than the chemistry step, is the rate-limiting step for multiple-turnover at 6×10^{-3} min^{-1}.

First-Order Rate Constant of Pre-Steady-State Cleavage (k_2). The cleavage rate constant under saturating ribozyme conditions ($k_2 = 0.91$ min^{-1}) in the minimal kinetic scheme is taken as the rate constant for the chemical conversion step. However, an alternative mechanism with an additional conformational change prior to the chemistry step cannot be excluded. In the latter case, the first-order rate constant k_2 could be the rate-limiting conformational change, or a combination of both conformational change and chemical conversion, and, as a result, the rate constant for chemical conversion would be even higher than 0.91 min^{-1}. However, the rate constant k_2 displayed a log-linear pH dependence with a slope of 1 in the pH range of 4.0−6.5, suggesting that the rate-limiting step involves a proton transfer (*15*). In addition, an identical pH profile was also observed with cleavage of the 2′,5′-linked substrate DS2, even though it has a rate constant (k_2) 100-fold slower than that of the normal substrate. The unchanged pH dependence suggests that the observed pH profile reflects an actual pK_a instead of a change in the rate-limiting step (*37*). If the observed k_2 represented a conformational change, a deprotonation step would have to be involved in this process.

The rate constant for the chemistry step (k_2, 0.91 min^{-1}) of ADC1 is slightly faster than the numbers reported for similar HDV antigenomic-derived ribozymes which associate with substrates through P1 base-pairing (*24*, *26*). However, this first-order rate constant is significantly slower than the rate constant for self-cleavage of naturally occurring autocatalytic HDV sequences. Depending on the sequence and cleavage conditions, the first-order rate constants for self-cleaving antigenomic sequences range up to 32 min^{-1} (*8*, *38*). With the fast-cleaving forms, the rate constant for self-cleavage is ~40-fold faster than that with the ADC1 *trans*-acting ribozyme under similar conditions. This significant difference might support the suggestion of a rate-limiting conformational change for *trans*-acting ribozymes. However, the pH dependence of self-cleavage showed a nearly identical bell-shaped profile to the one seen with *trans*-cleavage, except that both pK_a values were shifted upward about 0.5 pH unit (*11*; A. T. Perrotta and M.D.B., unpublished data). These data, together with the similar pH dependence of the 3′,5′- and 2′,5′-linked substrates (*15*), suggest that the difference in the rate constants could reflect the same rate-limiting step. It is possible that the active site in the *trans*-acting ribozyme is less rigidly structured relative to that of the *cis*-acting ribozyme, thus slowing the reaction.

Possibility of a Two-Step Substrate Binding Mechanism for the HDV Ribozyme. A mechanism that includes an intermediate binary complex (E·S)′ between the binding and chemistry step, as shown in Scheme 4, should also be considered for the HDV ribozyme because conformational change associated with substrate binding appear to be unavoidable. However we do not see evidence for a conformational change with the methods employed in this study. The apparent rate constants for substrate dissociation determined by pulse-chase experiments was calculated based on a single-exponential decay of the E·S complex. If a conformational change (e.g., helix docking) did occur, the apparent dissociation rate constant (k_{off}) would be $k_{off} \approx k_{-1}k_{-1}'/(k_{-1} + k_1' + k_{-1}')$, and the apparent binding constant would be (K_d/K_M') (*33*). The k_{off} would reduce to k_{-1} if the (E·S)′ complex was in a less favorable free energy state compared to the E·S complex (i.e., $k_{-1}' \gg k_1'$, k_{-1}); in that case the overall stability for a enzyme·substrate complex

(apparent binding constant = K_d) would be overestimated in our experiments. However, the apparent dissociation rate constant determined by the pulse-chase experiment was of the same order as the chemistry step k_2, which argues against the possibility of a much slower forward rate for conformational change. On the other hand, if the (E·S)′ complex is more stable than E·S (and $k_1' \gg k_{-1}'$, k_{-1}), the dissociation and association rate constants for substrate would be $k_{off} \approx k_{-1}k_{-1}'/k_1'$ and $k_{on} \approx k_1$[S], respectively, with overall stability for the enzyme·substrate complex of (K_d/K_M'). Although, there was no obvious biphasic binding observed in the pulse-chased experiments, a possible tertiary rearrangements cannot be omitted.

Contribution of the Adjacent 2′-OH Group at the Cleavage Site to Substrate Binding. Although the K_d for the substrate was estimated from the binding constant of a noncleavable analogue (DSA10), the number (58 nM) is in good agreement with the K_d obtained from k_1 and k_{-1} of substrate DS3 (62 nM), which were determined individually with chase experiments. This suggests that the adjacent 2′-OH group at the cleavage site does not contribute substantially to substrate binding. This was unexpected and in contrast to the hammerhead ribozyme, where the cleavage site 2′-OH group provides extra stabilization to the E·S complex. In that case a deoxynucleotide substitution 5′ to the cleavage site weakens substrate binding by a factor of 2 compared to the all-ribonucleotide substrate (*29*).

Significance of the Decreased Dissociation Equilibrium Constant of the Ribozyme Complexed with the Product Relative to the Substrate. For ADC1, the substrate associates with the ribozyme through 7 base pairs in P1 (Figure 1). The equilibrium dissociation constant of the substrate DS3 is ~60 nM, which corresponds to a binding energy (ΔG) of 10.3 kcal/mol under the reaction conditions. This number is close to the predicted value for an RNA duplex using free-energy parameters from a nearest-neighbor model in 1 M NaCl (predicted value = 10.2 kcal/mol) (*1*, *2*), suggesting that the interaction of the E·S complex might be simply through Watson−Crick base-pairing. However, the 3′ cleavage product, which associates with the ribozyme through the same base-pairing, showed a 24-fold decrease in its dissociation constant (K_d = 2.5 nM; ΔG = 12.3 kcal/mol). Stronger binding of the product oligonucleotide suggests extra stabilizing interactions in the product/ribozyme complex. From the crystal structure of the 3′ self-cleavage product of the genomic sequence, the 5′-OH leaving group is within H-bonding distance to the O2 (or N3) of cytosine 75 (C75) (C76 in the antigenomic sequence) (*9*). The free energy gained from an extra uncharged H-bond is estimated to be 0.5−1.8 kcal/mol (*39*−*41*), which would result in a factor of 2.3−15 decrease in the equilibrium dissociation constant. Also, due to the highly negative electrostatic environment of the active site (*9*), the neutral 5′-OH group of the product may be more stable than the negative-charged scissile phosphodiester bond. In this regard, it is important to note again that the 5′ cleavage product containing the cyclic phosphate appears to be bound very weakly if at all. Together these factors would appear favor cleavage.

Ground-state destabilization (*42*, *43*) has been demonstrated or proposed as a mechanism for ribozyme catalysis with several ribozymes, including the *Tetrahymena* group I ribozyme, RNase P, and some of the hammerhead ribozymes (*29*, *44*, *45*). For the HDV ribozyme, stronger binding of E·$P_{3'}$ relative to E·S complex may also indicate that ground-state destabilization contributes to catalysis. The mechanism could be analogous to the proposed mechanism for the *Tetrahymena* group I ribozyme (*45*). In that case a magnesium ion near the 3′ bridging oxygen of the scissile phosphodiester would be destabilizing in the ground state due to an unfavorable interaction to the electron-deficient 3′-oxygen; however, as negative charge develops on the 3′-oxygen at the transition state the interaction becomes favorable. Recently, a model for the mechanism of cleavage in the HDV ribozyme has been proposed by Nakano et al. (*12*), in which the protonated form of C75 (in genomic sequence, and its equivalent C76 in antigenomic), acting as a Brønsted acid, donates a proton to the 5′-oxygen leaving group. By analogy to the group I mechanism, in the ground state a positive charge on C75, situated near the 5′-bridging oxygen, would be unfavorable, but as negative charge developed on the 5′-oxygen this interaction would become more favorable. The difference in the dissociation equilibrium constants for substrate and product may be consistent with such a mechanism but needs to be tested further. Recently we have found that the equilibrium dissociation constants of substrates with different lengths of 5′ sequence increase slightly with increasing length from 1 to 5 nucleotides, accounting for another 3−6-fold increase in the binding constant of the E·S complex. This decrease in binding affinity of the substrates is strongly correlated to an increase in the rate for the chemical catalysis (I.-h. S., and M. D. B., unpublished data).

Association and Dissociation Rate Constants of the Substrate and Product. In addition to a large difference in thermodynamic stability, the substrate and product also demonstrated a difference in their association and dissociation rate constants. The association rate constant of the substrate DS3 and ribozyme ADC1 (2.1×10^7 M^{-1} min^{-1}) is at the lower limit of the rate constant for simple helix formation between two oligonucleotides (10^7−10^9 M^{-1} min^{-1}) (*46*−*51*). This value is close to that for hammerhead ribozymes with 13−16 bp of substrate binding [(1.0−8.5) $\times 10^7$ M^{-1} min^{-1}] (*29*, *52*) but not as fast as the helix formation step of the *Tetrahymena* ribozyme (2.4×10^8 M^{-1} min^{-1}) (*32*). The dissociation rate constant of a simple RNA helix is dependent on thermodynamic stability of the helix (*46*, *48*, *50*). For ADC1, the rate constant for substrate dissociation (1.4 min^{-1}) is within the range expected for this RNA duplex. However, for the 3′ cleavage product, the association and dissociation rate constants showed a 10-fold and 230-fold decrease, respectively, from those of the substrate DS3. The ratio of the fold decrease [$k_4/k_{-4} = K_{d(P3')}$] in the rate constants is consistent with the higher thermodynamic stability of the product (24-fold). Nevertheless, the product still demonstrates a 10-fold decrease in both association and dissociation rate constants compared to the substrate. Thus, the activation energy for both the association and dissociation of the substrate and ribozyme is 1.4 kcal/mol lower than that of the 3′ product, indicating a kinetically less stable E·S binary complex. This kinetic instability of the E·S complex suggests an intrinsically dynamic difference between these two binary complexes in addition to the thermodynamic differences described above.

Mechanism for Pre-Steady-State Cleavage of the HDV Ribozyme. The dissociation rate constant of the substrate is comparable to the rate constant of the chemistry step, indicating a Briggs−Haldane mechanism for HDV cleavage. According to the rate law, K_M' is $(k_{-1}+k_2)/k_1 = 105$ nM, and k_2/K_M' is $k_1k_2/(k_{-1}+k_2) = 8.5 \times 10^6$ M^{-1} min^{-1}, both of which are consistent with the numbers determined experimentally (Figure 3). This kinetic mechanism is similar to those observed with the RNase P, *Tetrahymena* (*28*), hairpin (*30*), and hammerhead ribozymes [except for HH8 (*29*, *52*)]. These enzymes, however, exhibit even slower substrate dissociation relative to the chemistry step such that every encounter with a substrate, the ribozyme converts it into products before it can dissociate.

Like other small ribozymes, there have been attempts to make use of *trans*-acting HDV ribozymes as therapeutic agents (*53*, *54*). With the HDV ribozyme, the faster substrate dissociation could allow better discrimination against substrates that are mispaired to the ribozyme, because a substrate forming a mismatch would be more likely to dissociate before proceeding to the chemistry step. Nevertheless, slow turnover due to strong binding of the 3′ cleavage product to the ribozyme may be detrimental for some applications.

HDV Cleavage of a 2′,5′-Linked Substrate Follows a Different Kinetic Mechanism from the Normal Substrate. The 2′,5-linked substrate is not cleaved by the ADC1 ribozyme in the presence of Ca^{2+} while the 3′,5′-linked substrate is cleaved slightly faster in Ca^{2+} than in Mg^{2+}. The change in the metal ion specificity upon simply altering the linkage at the cleavage site suggested a critical metal ion binding site close to the scissile phosphodiester bond for ADC1 catalysis. The cleavage mechanism of the 2′,5′-linked substrate confirms that the chemistry step is rate-limiting under ribozyme saturating conditions, which supports the hypothesis that the critical metal binding is required for the chemistry step, not merely for substrate binding. The pre-steady-state kinetics of the 2′,5′-linked substrate follows a Michaelis−Menten mechanism, in which substrate binding is at rapid equilibrium. This change in kinetic mechanism is the predicted outcome if the main effect of the altered linkage is to slow the chemistry step.

Do Elemental Rate Constants Measured under Pre-Steady-State Conditions Describe the Steady-State Cleavage Mechanism? An important test for the minimal kinetic scheme is whether it can describe the observed steady-state parameters. In multiple-turnover reactions, a burst amplitude stoichiometric with ribozyme concentration was observed, representing the first-turnover determined by rapid chemical conversion. The observed maximal rate constant (k_2) and apparent Michaelis constant (K_M') for the first turnover is in good agreement with numbers measured in single-turnover reactions. This initial burst was then followed by a linear phase, corresponding to the initial rate for steady-state kinetics. Under k_{cat} conditions (with saturating substrate), the rate-limiting step for multiple-turnover is dissociation of the 3′ cleavage product (0.0061 min^{-1}). Nevertheless, the second-order rate constant for the steady-state ADC1 cleavage, $k_{cat}/K_M = 7.6 \times 10^5$ M^{-1} min^{-1}, is 11-fold lower than that predicted from the single-turnover experiments, $k_2/K_M' = 8.3 \times 10^6$ M^{-1} min^{-1}. A similar situation has been seen with the RNase P ribozyme, where a slower second-order rate constant for the steady-state was caused by a slow conformational change of the ribozyme after dissociation of the mature tRNA (*3*). In that study, the plot of the initial velocity as a function of substrate concentration exhibited a steep increase at lower concentrations and obvious curvature at higher concentrations. However, such concentration dependence was not seen with ADC1 ribozyme[5] (Figure 8B). Another contribution to the lower second-order rate constant may be 3′ cleavage product inhibition. The 3′ product generated from the first turnover may act as a competitive inhibitor to substrate binding in the subsequent turnover. Therefore, product inhibition may give rise to an approximate 5-fold increase in apparent K_M but not effect the observed k_{cat}. Differences in the preincubation conditions may account for the other 2-fold difference between the predicted and measured second-order rate constants.

Reversibility of HDV Catalysis—Does Ligation Occur? Ligation of linear RNA monomers to circles during HDV replication is not yet fully understood. Unlike the hammerhead and hairpin ribozymes (*30*, *52*), the reverse reaction (ligation) has not been detected for either the genomic or the antigenomic HDV ribozymes. The recent structure (*9*) and the kinetic mechanism presented here reveal possible explanations for the elusive nature of the reverse reaction in HDV RNAs. First, there is no structural evidence for a candidate site in the ribozyme that could basepair with the sequence 5′ to the cleavage site. Second, the equilibrium dissociation constant of the 5′ cleavage product is not detectable, and the dissociation rate constant was estimated to be ≥ 12 min^{-1} using centrifuge columns. The external equilibrium (K_{eq}^{ext}) of the forward and reverse reactions can be described as follows:

$$K_{eq}^{ext} = (k_1k_2k_3k_4)/(k_{-1}k_{-2}k_{-3}k_{-4}) = K_{eq}^{int}[K_{d(P5')}K_{d(P3')}/K_{d(S)}]$$

in which K_{eq}^{int} represents the internal equilibrium of the chemistry step (k_2/k_{-2}); $K_{d(P5')}$, $K_{d(P3')}$, and $K_{d(S)}$ represent equilibrium dissociation constants of the 5′ cleavage product to the binary complex $E{\cdot}P_{3'}$, the 3′ product, and the substrate to the free enzyme, respectively (Figure 2). The equation shows that the external equilibrium is proportional to the ratio of $K_{d(P5')}$, $K_{d(P3')}$, and $K_{d(S)}$ [i.e., $K_{d(P5')}K_{d(P3')}/K_{d(S)}$], which has a upper limit of 10^{-8} M. Therefore, while presuming that the reverse reaction in internal equilibrium (k_{-2}) does occur, the external equilibrium is still limited by the extremely weak binding of the 5′ product to the $E{\cdot}P_{3'}$ complex.

ACKNOWLEDGMENT

We thank K. P. Bjornson and T. S. Wadkins for helpful comments on the manuscript and A. T. Perrotta for suggestions and sharing information.

REFERENCES

1. Freier, S. M., Kierzek, R., Jaeger, J. A., Sugimoto, N., Caruthers, M. H., Neilson, T., and Turner, D. H. (1986) *Proc. Natl. Acad. Sci. U.S.A. 83*, 9373−9377.

[5] For a kinetic mechanism involved in a conformational change after product release and prior to subsequent substrate binding, the concentration dependence of initial velocity can be described by the following equation: $v = (A[S] + B[S]^2)/(C + D[S] + [S]^2)$ (*3*). However, such a relation was not as clear for the HDV ribozyme because the second-order rate constants obtained from a fit to the equation [$A/C = (k_{cat}/K_M)_1 = 6.1 \times 10^5$ M^{-1} min^{-1}; $B/D = (k_{cat}/K_M)_2 = 1 \times 10^5$ M^{-1} min^{-1}; Figure 8B, dotted line] do not correspond to the second-order rate constants determined from single ($k_2/K_M' = 8.3 \times 10^6$ M^{-1} min^{-1})- and multiple-turnover (7.6×10^5 M^{-1} min^{-1}) reactions.

2. Turner, D. H., Sugimoto, N., Jaeger, J. A., Longfellow, C. E., Freier, S. M., and Kierzek, R. (1987) *Cold Spring Harbor Symp. Quant. Biol. LII*, 123−133.
3. Beebe, J. A., and Fierke, C. A. (1994) *Biochemistry 33*, 10294−10304.
4. Kuo, M. Y.-P., Sharmeen, L., Dinter-Gottleib, G., and Taylor, J. (1988) *J. Virol. 62*, 4439−4444.
5. Sharmeen, L., Kuo, M. Y.-P., Dinter-Gottlieb, G., and Taylor, J. (1988) *J. Virol. 62*, 2674−2679.
6. Wu, H.-N., Lin, Y.-J., Lin, F.-P., Makino, S., Chang, M.-F., and Lai, M. M. C. (1989) *Proc. Natl. Acad. Sci. U.S.A. 86*, 1831−1835.
7. Perrotta, A. T., and Been, M. D. (1990) *Nucleic Acids Res. 18*, 6821−6827.
8. Perrotta, A. T., and Been, M. D. (1991) *Nature 350*, 434−436.
9. Ferré-D'Amaré, A. R., Zhou, K., and Doudna, J. A. (1998) *Nature 395*, 567−574.
10. Wadkins, T. S., Perrotta, A. T., Ferré-D'Amaré, A. R., Doudna, J. A., and Been, M. D. (1999) *RNA 5*, 720−727.
11. Perrotta, A. T., Shih, I.-h., and Been, M. D. (1999) *Science 286*, 123−126.
12. Nakano, S.-I., Chadalavada, D. M., and Bevilacqua, P. C. (2000) *Science 287*, 1493−1497.
13. Kuo, M. Y.-P., Goldberg, J., Coates, L., Mason, W., Gerin, J., and Taylor, J. (1988) *J. Virol. 62*, 1855−1861.
14. Suh, Y.-A., Kumar, P. K. R., Taira, K., and Nishikawa, S. (1993) *Nucleic Acids Res. 21*, 3277−3280.
15. Shih, I.-h., and Been, M. D. (1999) *RNA 5*, 1140−1148.
16. Been, M. D., Perrotta, A. T., and Rosenstein, S. P. (1992) *Biochemistry 31*, 11843−11852.
17. Been, M. D. (1994) *Trends Biochem. Sci. 19*, 251−256.
18. Puttaraju, M., Perrotta, A., and Been, M. (1993) *Nucleic Acids Res. 21*, 4253−4258.
19. Perrotta, A. T., and Been, M. D. (1992) *Biochemistry 31*, 16−21.
20. Nishikawa, F., Kawakami, J., Chiba, A., Shirai, M., Kumar, P. K., and Nishikawa, S. (1996) *Eur. J. Biochem. 237*, 712−718.
21. Cech, T. R. (1993) in *The RNA World*, pp 239−269, Cold Spring Harbor Laboratory Press, Plainview, NY.
22. Long, D. M., and Uhlenbeck, O. C. (1993) *FASEB J. 7*, 25−30.
23. Symons, R. H. (1992) *Annu. Rev. Biochem. 61*, 641−671.
24. Mercure, S., Lafontaine, D., Annaanvoranich, S., and Perreault, J.-P. (1998) *Biochemistry 37*, 16975−16982.
25. Fauzi, H., Kawakami, J., Nishikawa, F., and Nishikawa, S. (1997) *Nucleic Acids Res. 25*, 3124−3130.
26. Bravo, C., Lescure, F., Laugâa, P., Fourrey, J.-L., and Favre, A. (1996) *Nucleic Acids Res. 24*, 1351−1360.
27. Davanloo, P., Rosenberg, A. H., Dunn, J. J., and Studier, F. W. (1984) *Proc. Natl. Acad. Sci. U.S.A. 81*, 2035−2039.
28. Herschlag, D., and Cech, T. R. (1990) *Biochemistry 29*, 10159−10171.
29. Fedor, M. J., and Uhlenbeck, O. C. (1992) *Biochemistry 31*, 12042−12054.
30. Hegg, L. A., and Fedor, F. J. (1995) *Biochemistry 34*, 15813−15828.
31. Rose, I. A. (1980) *Methods Enzymol. 64*, 47−59.
32. Bevilacqua, P. C., Kierzek, R., Johnson, K. A., and Turner, D. H. (1992) *Science 258*, 1355−1358.
33. Johnson, K. A. (1992) in *The Enzymes* (Boyer, P. D., Ed.) pp 1−61, Academic Press, New York.
34. Barshop, B. A., Wrenn, R. F., and Frieden, C. (1983) *Analytic Biochemistry 130*, 134−135.
35. Lee, C.-B., Lai, Y.-C., Ping, Y.-H., Huang, Z.-S., Lin, J.-Y., and Wu, H.-N. (1996) *Biochemistry 35*, 12303−12312.
36. Ferscht, A. (1985) *Enzyme Structure and Mechanism*, 2nd ed., W. H. Freeman and Company, New York.
37. Herschlag, D., and Khosla, M. (1994) *Biochemistry 33*, 5291−5297.
38. Perrotta, A. T., and Been, M. D. (1998) *J. Mol. Biol. 279*, 361−373.
39. Silverman, S. K., and Cech, T. R. (1999) *Biochemistry 38*, 8691−8702.
40. Fersht, A. R., Shi, J. P., Knill-Jones, J., Lowe, D. M., Wilkinson, A. J., Blow, D. M., Brick, P., Carter, P., Waye, M. M., and Winter, G. (1985) *Nature 314*, 235−238.
41. Fersht, A. R. (1987) *Trends Biochem. Sci. 12*, 301−304.
42. Haldane, J. B. S. (1930) *Enzymes*, Longmans, Green and Co., London.
43. Kraut, J. (1988) *Science 242*, 533−540.
44. Crary, S. M., Niranjanakumari, S., and Fierke, C. A. (1998) *Biochemistry 37*, 9409−9416.
45. Narlikar, G. J., Gopalakrishnan, R. S., McConnell, R. S., Usman, N., and Herschlag, D. (1995) *Proc. Natl. Acad. Sci. U.S.A. 92*, 3668−3672.
46. Craig, M. E., Crothers, D. M., and Doty, P. (1971) *J. Mol. Biol. 62*, 383−401.
47. Nelson, J. W., Martin, F. H., and Tinoco, I. J. (1981) *Biopolymers 20*, 2509−2531.
48. Porschke, D., and Eigen, M. (1971) *J. Mol. Biol. 62*, 361−381.
49. Ravetch, J., Gralla, J., and Crothers, D. M. (1974) *Nucleic Acids Res. 1*, 109−127.
50. Porschke, D., Uhlenbeck, O. C., and Martin, F. H. (1973) *Biopolymers 12*, 1313−1335.
51. Breslauer, K. J., and Bina-Stein, M. (1977) *Biophys. Chem. 71*, 211−216.
52. Hertel, K., Herschlag, D., and Uhlenbeck, O. C. (1994) *Biochemistry 33*, 3374−3385.
53. Roy, G., Ananvoranich, S., and Perreault, J. P. (1999) *Nucleic Acids Res. 27*, 942−948.
54. Madejon, A., Bartolome, J., and Carreno, V. (1998) *J. Hepatol. 29*, 385−393.

BI000499+